Magnetotransport in two-dimensional electron systems with spin-orbit interaction

M. Langenbuch,* M. Suhrke,† and U. Rössler
Institut für Theoretische Physik - Universität Regensburg, 93040 Regensburg, Germany
(Received 11 April 2003; revised manuscript received 6 October 2003; published 4 March 2004)

We present magnetotransport calculations for homogeneous two-dimensional electron systems including the Rashba spin-orbit interaction, which mixes the spin eigenstates and leads to a modified fan chart with crossing Landau levels. The quantum mechanical Kubo formula is evaluated by taking into account spin-conserving scatterers in an extension of the self-consistent Born approximation that considers the spin degree of freedom. The calculated conductivity exhibits besides the well-known beating in the Shubnikov–de Haas (SdH) oscillations, a modulation which is due to a suppression of scattering away from the crossing points of Landau levels and does not show up in the density of states. This modulation, surviving even at elevated temperatures when the SdH oscillations are damped out, could serve to identify spin-orbit coupling in magnetotransport experiments. Our magnetotransport calculations are extended also to lateral superlattices and predictions are made with respect to $1/B$ periodic oscillations in dependence on carrier density and strength of the spin-orbit coupling.

DOI: 10.1103/PhysRevB.69.125303 PACS number(s): 73.23.−b, 72.20.−i, 85.75.−d

I. INTRODUCTION

The Rashba spin-orbit (SO) coupling[1,2] that exists in systems with axial symmetry, plays a key role in spintronics[3] realized with two-dimensional (2D) carriers in semiconductor heterostructures as it allows one to manipulate the spin by a gate-controlled confinement potential. Spin-orbit coupling mixes the spin states and removes the spin degeneracy for states with finite momentum. Besides the Rashba term caused by the asymmetry of the confinement, there exists also a SO coupling due to the inversion asymmetry of the crystalline structure of the semiconductor bulk material (Dresselhaus term[4]). Both types of SO coupling combine to an anisotropic spin-splitting of 2D electrons, which has been analyzed by inelastic light scattering[5] and plays a role also in weak localization studies.[6,7] The intimate relation between spin splitting and spin relaxation, well known for bulk material,[8,9] has found renewed interest for 2D electrons,[10,11] furthered by the possibility to measure spin-relaxation times with monopolar optical orientation.[12] The zero-field spin splitting[13] has to compete with the Zeeman spin splitting if a magnetic field is applied perpendicular to the plane of the 2D electron system. This results in a fan chart showing characteristic crossings of Landau levels, which in magnetotransport data are detected as beating of the Shubnikov–de Haas (SdH) oscillations.[14–17] The two SO coupling mechanisms have been found to be responsible for anomalous magneto oscillations.[18–20] The structural asymmetry of the confinement can be tuned into a regime where the Rashba SO coupling dominates over the bulk inversion asymmetry.[13] In spite of this current interest in the Rashba SO coupling and its relevance for spin-related transport in two-dimensional electron systems (2DES) it is surprising that there is so far no rigorous magnetotransport calculation which takes this coupling into account.

Here, we present fully quantum-mechanical calculations of the magnetoconductivity including the Rashba SO interaction. The calculations are based on the evaluation of the Kubo formula with an extension of the self-consistent Born approximation (SCBA) by taking into account the electron spin degree of freedom. Our results show besides the known beats in the SdH oscillations an additional modulation connected with the crossing of Landau levels. This modulation, which is not seen in the density of states, arises as we take into account spin-conserving impurity scattering which is suppressed when the SO coupled states are not degenerate. It survives even at higher temperatures, when SdH oscillations have died out, and could serve, if experimentally detected, as another fingerprint of SO interaction. In lateral superlattices,[22] where a 2DES is subjected to a periodic potential, there exist besides the SdH oscillations other $1/B$ periodic magnetotransport oscillations due to commensurability between cyclotron radius and lattice constant[23] and due to the formation of a miniband structure.[24,25] From our magnetotransport calculations for lateral superlattices with weak one-dimensional (1D) modulation we predict a splitting of these periods due to SO coupling and calculate their dependence on its strength and carrier density.[26,27]

The paper is organized as follows. In Sec. II we describe the energy spectrum and eigenstates of a 2DES with Rashba SO interaction. For the calculation of the conductivity we simplify the energy spectrum and introduce a constant SO splitting model. In Sec. III the SCBA is extended by the spin degree of freedom to describe the scattering of spin-conserving impurities in a 2DES with SO interaction. The effects of this extension will be demonstrated for a two-level system: It will turn out that for SO coupled states the scattering, which is strongest for degenerate levels, is reduced when separating these levels. In Sec. IV we present the conductivity and compare the cases with and without SO coupling. Finally in Sec. V we show results for a system with SO interaction and a 1D periodic modulation and study in the power spectrum of the magnetoconductivity the evolution of the characteristic periods with increasing SO coupling.

 ©2004 The American Physical Society

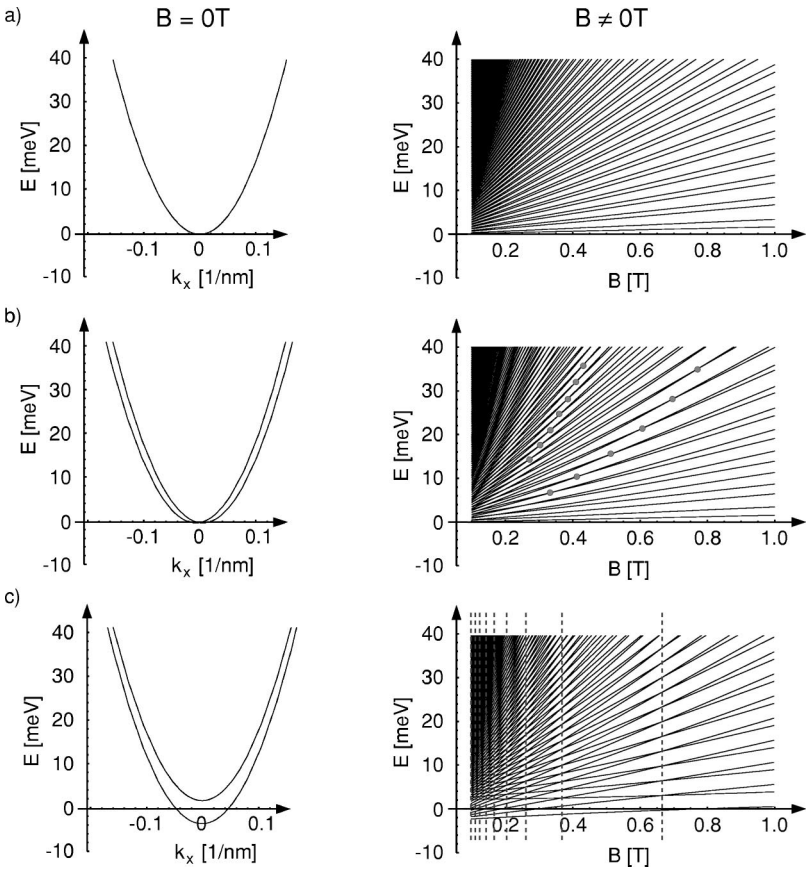

FIG. 1. Subband energy dispersion (left) and Landau levels (right) of a 2DES (parameters $m^*=0.023\,m_0$, $g^*=-14.9$ correspond to InAs) (a) without SO coupling $\alpha_z=0$ eVm, (b) with SO coupling $\alpha_z=2.0\times10^{-11}$ eVm, and (c) with constant SO splitting $\overline{\alpha_z}=2.5$ meV.

II. ENERGY SPECTRUM AND THE CONSTANT SPIN-ORBIT SPLITTING MODEL

The Hamiltonian of a 2DES (in the xy plane) realized in the lowest subband of a semiconductor heterostructure with effective mass m^*, Rashba SO interaction due to the z confinement with coupling constant α_z, and Zeeman term with effective g factor g^*, in a magnetic field $\mathbf{B}=B\hat{\mathbf{e}}_z$, is given by

$$H=\frac{1}{2m^*}(\pi_x^2+\pi_y^2)-\frac{\alpha_z}{\hbar}(\sigma_x\pi_y-\sigma_y\pi_x)+\frac{1}{2}g^*\mu_B\sigma_z B, \tag{1}$$

where π_μ denotes the kinetic momentum and σ_μ the Pauli spin matrices, $\mu\in\{x,y,z\}$. The spin (*up/down*) is quantized in z direction. The energy spectrum is isotropic and without the magnetic field, $B=0$, it depends on the wave vector $\boldsymbol{k}$ and is given by[1]

$$E_{\boldsymbol{k}}^{\pm}=\frac{\hbar^2\boldsymbol{k}^2}{2m^*}\pm\alpha_z|\boldsymbol{k}|. \tag{2}$$

The SO coupling lifts the spin degeneracy even without external magnetic field and the energy branches are split by

$$\Delta_{\mathrm{SO}}=2\alpha_z|\boldsymbol{k}|. \tag{3}$$

Including the external magnetic field, the Hamiltonian can be formulated with ladder operators $a^\dagger|n\rangle=\sqrt{n+1}\,|n+1\rangle$, $a|n\rangle=\sqrt{n}\,|n-1\rangle$. In the Pauli representation the Hamiltonian can be written as

$$H=\hbar\omega_c\begin{pmatrix} a^\dagger a+\frac{1}{2}+\beta & \alpha a \\ \alpha a^\dagger & a^\dagger a+\frac{1}{2}-\beta \end{pmatrix} \tag{4}$$

with the parameters $\beta=g^*\mu_B B/2\hbar\omega_c$ and $\alpha=-\alpha_z\sqrt{2}/\lambda_c\hbar\omega_c$, the cyclotron frequency $\omega_c=eB/m^*$ and the magnetic length $\lambda_c=(\hbar/eB)^{1/2}$.

In Fig. 1 we show the spectrum of Hamiltonian (1) without magnetic field (left) and with magnetic field (right) for parameter values corresponding to InAs ($m^*=0.023\,m_0, g^*=-14.9$). In Fig. 1(a) the situation without SO coupling with spin-degenerate parabolic dispersion (left) and regular fan chart of Landau levels (right) is depicted. Including SO coupling the picture of Fig. 1(b) is obtained with the k dependent splitting of the subband dispersion (left) and the characteristic crossing pattern of Landau levels (right). For this calculation the SO coupling parameter α_z was chosen to be $\alpha_z=2.0\times10^{-11}$ eVm close to the experimental values reported for InAs samples.[14] The Hamiltonian (4) indicates that in the presence of SO coupling the spin states, quantized in z direction and used in the Pauli representation, are no longer eigenstates. Instead Hamiltonian (4) is diagonal for the states[1]

$$|n,r\rangle=\begin{pmatrix} c^u_{nr}\Phi_n \\ c^d_{nr}\Phi_{n+1}\end{pmatrix} \text{and } |n,l\rangle=\begin{pmatrix} c^u_{nl}\Phi_{n-1} \\ c^d_{nl}\Phi_n\end{pmatrix}, \tag{5}$$

which can be classified by the helicity $\kappa\in\{\text{right,left}\}$ and the Landau index $n=0,1,2,\ldots$. Φ_n are the eigenfunctions of the harmonic oscillator. These *right*/*left* states evolve with increasing SO coupling from the spin *up*/*down* states, respectively, by the following choice of the coefficients:

$$c^u_{nr}=\frac{\alpha\sqrt{n+1}}{\sqrt{(n+1)\alpha^2+\left(\left(\frac{1}{2}-\beta\right)-\sqrt{d_r}\right)^2}},$$

$$c^d_{nr}=\frac{\left(\frac{1}{2}-\beta-\sqrt{d_r}\right)}{\sqrt{(n+1)\alpha^2+\left(\left(\frac{1}{2}-\beta\right)-\sqrt{d_r}\right)^2}}, \tag{6}$$

for the right states and

$$c^u_{nl}=\frac{\alpha\sqrt{n}}{\sqrt{n\alpha^2+\left(\left(\frac{1}{2}-\beta\right)+\sqrt{d_l}\right)^2}},$$

$$c^d_{nl}=\frac{\left(\frac{1}{2}-\beta+\sqrt{d_l}\right)}{\sqrt{n\alpha^2+\left(\left(\frac{1}{2}-\beta\right)+\sqrt{d_l}\right)^2}}, \tag{7}$$

for left states with $d_r=\sqrt{(n+1)\alpha^2+(\frac{1}{2}-\beta)^2}$ and $d_l=\sqrt{n\alpha^2+(\frac{1}{2}-\beta)^2}$. The energy eigenvalues of these states are

$$E_{nr}=\hbar\omega_c\left(1+n-\sqrt{(n+1)\alpha^2+\left(\frac{1}{2}-\beta\right)^2}\right), \tag{8}$$

$$E_{nl}=\hbar\omega_c\left(n+\sqrt{n\alpha^2+\left(\frac{1}{2}-\beta\right)^2}\right). \tag{9}$$

In the following we use the notation

$$|n,\kappa\rangle=\sum_\sigma c^\sigma_{n\kappa}\left|n-\frac{\sigma-\kappa}{2},\sigma\right\rangle, \tag{10}$$

where σ denotes the spin quantized in z direction (1: up, -1: down) and κ the helicity (1: right, -1: left).

The low-temperature magnetoconductivity is determined by the electron states close to the Fermi energy. To simplify the energy spectrum and the spinor coefficients we eliminate the k dependence of the SO splitting. For vanishing magnetic field the energy dispersion for a constant SO splitting model[28] is

$$E=\frac{\hbar^2k^2}{2m^*}\pm\frac{1}{2}\Delta_{SO}, \tag{11}$$

shown in Fig. 2(c) (left). For fixed energy the two solutions with the same direction of the k vector exhibit different slopes of the energy dispersion but for energies much higher than Δ_{SO} this difference is negligible. For the spectrum with magnetic field we divide the SO coupling constant by the absolute value of $\boldsymbol{k}$ and replace $\alpha\to\overline{\alpha}/\sqrt{a^\dagger a+\frac{1}{2}}$ with $\overline{\alpha}=\overline{\alpha_z}/2\hbar\omega_c$, where $\overline{\alpha_z}=\frac{1}{2}\Delta_{SO}$ is taken from the spin splitting Δ_{SO} at the Fermi energy. We will be interested mainly in the low-magnetic-field regime where the conductivity is dominated by contributions from Landau levels with $n\gg1$ so we arrive with the approximation $n+1/n\to1$ at a model with constant spin-orbit splitting and the coefficients (6) and (7) take the forms

$$c^u_r=\frac{\overline{\alpha}}{\sqrt{\overline{\alpha}^2+\left(\left(\frac{1}{2}-\beta\right)-\sqrt{\overline{d}}\right)^2}},$$

$$c^d_r=\frac{\left(\frac{1}{2}-\beta-\sqrt{\overline{d}}\right)}{\sqrt{\overline{\alpha}^2+\left(\left(\frac{1}{2}-\beta\right)-\sqrt{\overline{d}}\right)^2}} \tag{12}$$

and

$$c^u_l=\frac{\overline{\alpha}}{\sqrt{\overline{\alpha}^2+\left(\left(\frac{1}{2}-\beta\right)+\sqrt{\overline{d}}\right)^2}},$$

$$c^d_l=\frac{\left(\frac{1}{2}-\beta+\sqrt{\overline{d}}\right)}{\sqrt{\overline{\alpha}^2+\left(\left(\frac{1}{2}-\beta\right)+\sqrt{\overline{d}}\right)^2}} \tag{13}$$

respectively, where $\overline{d}=\sqrt{\overline{\alpha}^2+(\frac{1}{2}-\beta)^2}$. For this constant SO splitting model the energy eigenvalues are

$$E_{nr}=\hbar\omega_c\left(1+n-\sqrt{\overline{\alpha}^2+\left(\frac{1}{2}-\beta\right)^2}\right), \tag{14}$$

$$E_{nl}=\hbar\omega_c\left(n+\sqrt{\overline{\alpha}^2+\left(\frac{1}{2}-\beta\right)^2}\right). \tag{15}$$

The energy spectrum of this model [Fig. 1(c)] consists of the two branches of right and left states which by our choice of $\overline{\alpha_z}$ are shifted by $\Delta_{SO}=5$ meV. The crossing of Landau levels takes place for all levels at the same magnetic field. Thus our model preserves the two main effects of SO coupling, the crossing of Landau levels and the mixing of spin components up/down.

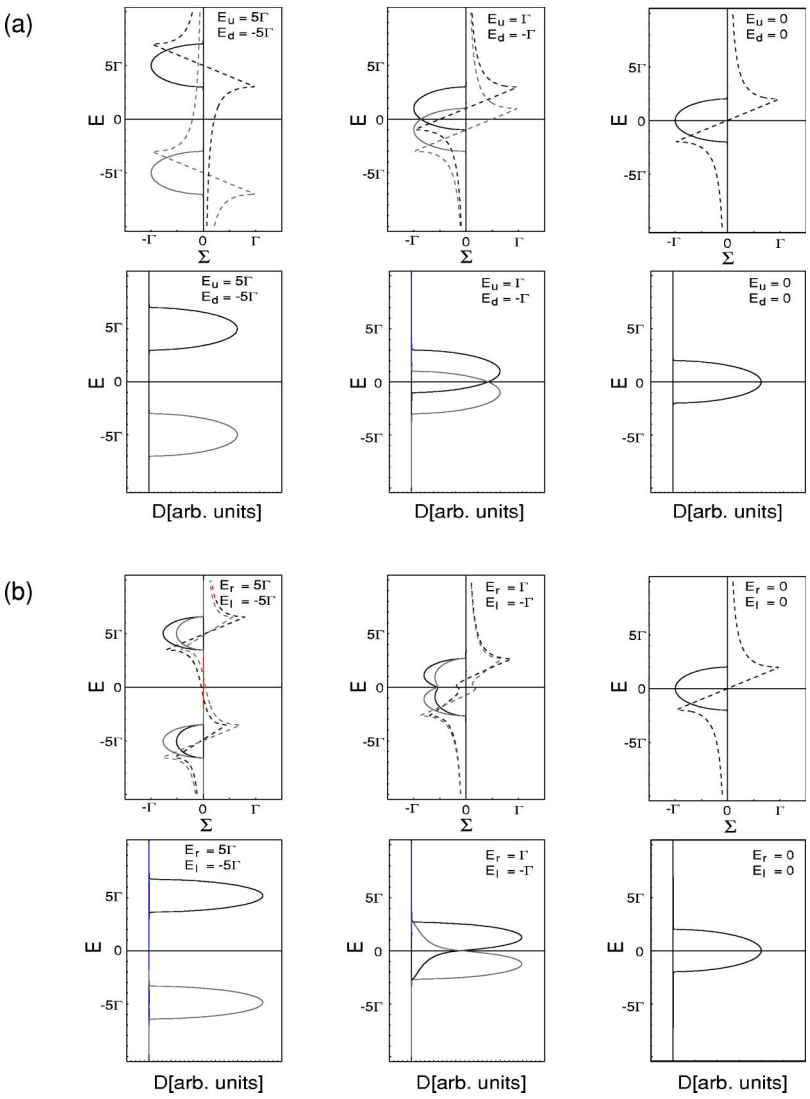

FIG. 2. Self-energies $\Sigma(E)$ (real and imaginary parts as dashed and solid lines, respectively) and density of states for a two-level system without (a) and with (b) SO coupling for different separation of the up/down or right/left eigenstates in (a) and (b), respectively. In (b) a mixing coefficient $\alpha_{\kappa\kappa}=0.6$ at the energies E_r and E_l has been chosen.

III. SCBA WITH SPIN DEGREE OF FREEDOM

For the calculation of the conductivity scattering has to be taken into account. The impurity-averaged Green function of the system G is given by the Dyson equation

$$G = G_0 + G_0 \Sigma G. \tag{16}$$

The scattering is included by the self-energy Σ in SCBA.[29] The matrix elements of the self-energy $\langle\alpha|\Sigma|\alpha'\rangle = \Sigma_{\alpha\alpha'}$, $\alpha=(n\kappa)$ read in the basis of eigenstates (10)

$$\Sigma_{\alpha\alpha'} = \sum_{\beta\beta'} \Gamma_{\alpha\beta\beta'\alpha'} G_{\beta\beta'}. \tag{17}$$

The kernel $\Gamma_{\alpha\beta\beta'\alpha'}$ is given by the expression

$$\Gamma_{\alpha\beta\beta'\alpha'} = \int \frac{dq^2}{(2\pi)^2} |\tilde{v}_I(\boldsymbol{q})|^2 \langle\alpha|e^{i\boldsymbol{qr}}|\beta\rangle\langle\beta'|e^{-i\boldsymbol{qr}}|\alpha'\rangle, \tag{18}$$

where $\tilde{v}_I(\boldsymbol{q})$ denotes the Fourier transform of the impurity potential.[30]

We consider spin-conserving short-range impurity scattering. By this choice we neglect magnetic impurities and SO coupling with the scattering center, thus without Rashba SO coupling scattering is possible only between states with the same spin quantum number. In the new basis (10), including the Rashba term, scattering between states with different helicity becomes possible. For δ scatterers Eq. (18) simplifies to

$$\Gamma_{\alpha\beta\beta'\alpha'} = \Gamma^2 \sum_{\sigma\sigma'} (c^{\sigma}_{n\kappa})^* c^{\sigma}_{m\tilde{\kappa}} (c^{\sigma'}_{m'\tilde{\kappa}'})^* c^{\sigma'}_{n'\kappa'} \tag{19}$$

$$\times \delta_{n-(\sigma-\kappa/2),n'-(\sigma'-\kappa'/2)} \delta_{m-(\sigma-\tilde{\kappa}/2),m'-(\sigma'-\tilde{\kappa}'/2)}, \tag{20}$$

where $\Gamma^2=(1/2\pi)\hbar\omega_c\hbar/\tau$ is connected through the relaxation time τ with the mobility $\mu=e\tau/m^*$ in the case without magnetic field. The Kronecker symbols have the form $\delta_{n',n-\theta}$ and $\delta_{m',m-\mu}$ with $\theta=\frac{1}{2}(\sigma-\sigma'-\kappa+\kappa')=-2,-1,0,1,2$ and $\mu=\frac{1}{2}(\sigma-\sigma'-\tilde{\kappa}+\tilde{\kappa}')=-2,-1,0,1,2$. We restrict ourselves to the diagonal approximation in the spacial quantum numbers by considering only $\theta=\mu=0$. In this ap-

proximation the self-energy reads $\Sigma_{nn'}^{\kappa\kappa'}=\Sigma^{\kappa\kappa'}\delta_{nn'}$ with $\Sigma^{\kappa\kappa'}$ independent of n, and the Green function $G_{mm'}^{\kappa\kappa'}=G_m^{\kappa\kappa'}\delta_{mm'}$. Thus the SCBA self-energy becomes

$$\Sigma^{\kappa\kappa'}=\Gamma^2\sum_m \sum_{\tilde{\kappa}\tilde{\kappa}'} \alpha_{\kappa\tilde{\kappa}\kappa'\tilde{\kappa}'}^{\kappa\kappa'} G_m^{\tilde{\kappa}\tilde{\kappa}'} \tag{21}$$

with

$$\alpha_{\kappa\tilde{\kappa}\kappa'\tilde{\kappa}'}^{\kappa\kappa'}=\sum_{\sigma\sigma'} (c_\kappa^\sigma)^* c_{\tilde{\kappa}}^\sigma (c_{\tilde{\kappa}'}^{\sigma'})^* c_{\kappa'}^{\sigma'} \delta_{\sigma-\sigma',\kappa-\kappa'}\delta_{\sigma-\sigma',\tilde{\kappa}-\tilde{\kappa}'} \tag{22}$$

and

$$(G_m^{\kappa\kappa'})^{-1}=(G_{0\,m}^{\kappa})^{-1}\delta_{\kappa\kappa'}-\Sigma^{\kappa\kappa'}, \tag{23}$$

where $G_{0\,m}^{\kappa}$ is the Green function of the system without impurities. Using the abbreviations $\Sigma^{\kappa\kappa}\equiv\Sigma^{\kappa}$, $G_m^{\kappa\kappa}\equiv G_m^{\kappa}$ and $\alpha_{\kappa\tilde{\kappa}\kappa'\tilde{\kappa}'}^{\kappa\kappa}\equiv\alpha_{\kappa\tilde{\kappa}}\delta_{\kappa\tilde{\kappa}'}$ the self-energy can now be calculated from

$$\Sigma^{\kappa}=\Gamma^2\sum_{m\tilde{\kappa}} \alpha_{\kappa\tilde{\kappa}} G_m^{\tilde{\kappa}} \quad \text{with} \quad \alpha_{\kappa\tilde{\kappa}}=\sum_\sigma |c_\kappa^\sigma|^2|c_{\tilde{\kappa}}^\sigma|^2. \tag{24}$$

The off-diagonal elements of the self-energy will be neglected.

The density of states for the left and right components is obtained by the trace over the spectral functions $A_m^\kappa=-\mathrm{Im}\{1/\pi\ G_m^\kappa\}$.

$$D^\kappa(E)=\frac{1}{L_xL_y}\mathrm{Tr}_m\{A_m^\kappa\}$$

$$=-\frac{1}{(\pi\lambda_c\Gamma)^2}\sum_{\kappa'} (\alpha^{-1})_{\kappa\kappa'}\mathrm{Im}\{\Sigma^{\kappa'}(E)\}. \tag{25}$$

Here $(\alpha^{-1})_{\kappa\kappa'}$ are the elements of the inverse of the matrix formed from the $\alpha_{\kappa\kappa'}$ of Eq. (24) for which $\alpha_{\kappa\kappa}+\alpha_{\kappa(-\kappa)}=1$. For vanishing SO coupling one has $\alpha_{\kappa\tilde{\kappa}}\to\delta_{\kappa\tilde{\kappa}}$ and the standard SCBA result is reproduced. For strong SO coupling if $\bar{\alpha}>1$, i.e., the Landau splitting is smaller than the splitting induced by the SO interaction, one has $\alpha_{\kappa\tilde{\kappa}}\to\frac{1}{2}$.

Due to the SO interaction the Landau levels of different helicity cross as seen in Fig. 1(b) and 1(c). To demonstrate the influence of scattering around these crossing points we apply the described extension of the SCBA to a two-level system with different spacings. The two states at the energies E_r, E_l have different helicity and evolve with increasing SO coupling from the spin *up*/*down* states with energy E_u and E_d.

Without SO interaction [Fig. 2(a)] we have $\alpha_{\kappa\tilde{\kappa}}=\delta_{\kappa\tilde{\kappa}}$ and the two levels E_u and E_d are pure spin states. In the upper (lower) panels of Fig. 2(a) the evolution of the self-energy (density of states) is shown for decreasing level separation E_u-E_d. It is clearly seen that the form of these quantities does not change with the level separation. In contrast, for finite SO coupling [Fig. 2(b)] the situation is completely different. The self-energies of the two levels E_r and E_l (now being a mixture of pure spin states) are reduced as compared with Fig. 2(a) but have significant contributions at the energy of the state with opposite helicity, while the density of states gets more concentrated at the level energies. For strongly SO coupled states $\alpha_{\kappa\kappa}\to\frac{1}{2}$ the height and width of the imaginary part of the self-energy are reduced by a factor of $\sqrt{2}$ for $E_l-E_r\gg\Gamma$, as can be seen by inspection of Eq. (24). With decreasing level separation the results of Fig. 2(a) (right panels) are recovered. As the imaginary part of the self-energy is inversely proportional to the relaxation time we conclude, that the SO coupling becomes effective by reducing the scattering efficiency (or increasing the corresponding transport times) for nondegenerate states of different helicity away from the crossing points of the full spectrum [Fig. 1(b) and 1(c)]. This will become important in the calculations of the conductivity (Sec. IV).

To summarize, the scattering strength depends on the level separation, i.e., on the distance from crossing points in Fig. 1. As this distance varies with the magnetic field we expect a modulation of the scattering strength with the magnetic field.

IV. CONDUCTIVITY

Based on the exact eigenstates of the constant SO splitting model we evaluate the Kubo formula

$$\sigma_{\mu\mu}=\frac{e^2\pi\hbar}{L_xL_y}\int dE\left(-\frac{df_0}{dE}\right)\sum_{\alpha\alpha'} |\langle\alpha|v_\mu|\alpha'\rangle|^2 A_\alpha A_{\alpha'}, \tag{26}$$

to calculate the conductivity. Here the spectral function A_α includes the impurity scattering in SCBA as described in Sec. III and the Fermi distribution function yields the temperature average. The velocity is given by the equation $i\hbar v_\mu=[x_\mu,H]$, which results in

$$v_x=\frac{1}{m^*}\left(\pi_x+\frac{\alpha_z}{\hbar}\sigma_y\right) \quad \text{and} \quad v_y=\frac{1}{m^*}\left(\pi_y-\frac{\alpha_z}{\hbar}\sigma_x\right). \tag{27}$$

Besides $\sigma_{\mu\mu},\mu=x,y$ we calculate also the thermodynamic density of states at the Fermi energy $D_\mathrm{F}=\int dE(-df_0/dE)D(E)$. In Fig. 3 both quantities are shown for the two temperatures $T=1$ K and $T=3$ K with the Fermi energy determined from the constant electron density n_s. For comparison the classical high-temperature limit of the SCBA for decoupled Landau levels is given by the dashed line. The effect of SO coupling is seen in D_F as beating pattern, well known from measured SdH oscillations,[14–17] while in σ_{xx} it causes an additional modulation, which survives even at a higher temperature when the SdH oscillations are damped out. The period of this modulation is determined by the crossing of Landau levels (marked in Fig. 3) induced by the SO coupling. The self-energy enters differently into D_F and σ_{xx}. In D_F it leads to a modulated broadening of the Landau levels which is washed out in the high-temperature limit, while in σ_{xx} it acts in addition as a scattering time whose dependence on the level separation remains even at higher temperatures. This is seen by comparing with the classical SCBA limit for decoupled Landau levels (dashed line): the

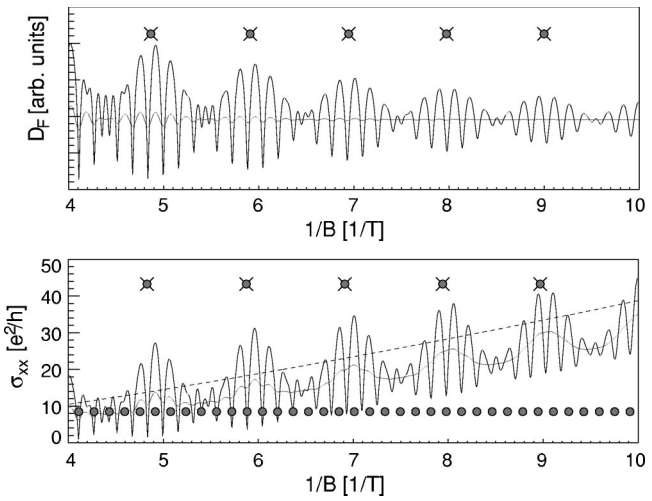

FIG. 3. Thermodynamic density of states at the Fermi energy D_F and longitudinal conductivity σ_{xx} for the parameters of Fig. 1, electron density $n_s = 3.0 \times 10^{15}$ m^{-2} and mobility $\mu = 50$ m^2/Vs at two temperatures $T = 1.0$ K (black solid) and 3.0 K (gray solid). The gray circles mark the expected position of maxima of the SdH oscillations without SO coupling, Landau-level crossings due to the SO coupling are indicated by crosses. The dashed line in the plot of the longitudinal conductivity is the classical limit of the SCBA when the Landau levels are decoupled.

Kubo formula (26) yields a magnetoconductivity which is reduced away from the crossing points due to suppression of impurity scattering. (Note, that we are in the limit $\omega_c \tau \gg 1$, where the Drude conductivity is proportional to $1/\tau$.) The influence of the modified SCBA, which in Sec. III and Fig. 2(a) has been demonstrated for the self-energy, will now be shown for the conductivity which in Fig. 4 is depicted in dependence on the mixing coefficient $\alpha_{\kappa\tilde{\kappa}}$. We keep the energy spectrum with SO splitting unchanged and analogous to the two-level system we vary $\alpha_{\kappa\kappa}$, which otherwise is given by the coefficients c_κ^σ. Neglecting the scattering between states of different helicity $\alpha_{\kappa\kappa} = 1$, the crossing of Landau levels has no effect on the conductivity. For dominant SO coupling, $\alpha_{\kappa\kappa} \to \frac{1}{2}$, we see that the conductivity is reduced between crossing points of Landau levels. We can distinguish two situations (top of Fig. 4). The states with different helicity are degenerate (A) and the scattering efficiency keeps unchanged; when right/left states are not degenerate (B) the conductivity depends on $\alpha_{\kappa\tilde{\kappa}}$. In Fig. 5, we have varied the strength of the impurity scattering by changing the parameter Γ. At the classical limit of the SCBA with decoupled Landau levels (dashed lines) we see that the conductivity rises with increasing Γ. The modulation of the conductivity due to the crossing of Landau levels decreases, because the limit of decoupled Landau levels can no longer be reached for large enough Γ.

We have shown by a quantum-mechanical calculation, that the SO coupling causes the expected beats of the SdH oscillations. In addition our results exhibit a modulation of the magnetoconductivity which can be ascribed to a modification of impurity scattering in the presence of SO coupling. This could help in experiments to distinguish the effect of the SO coupling from that of inhomogeneous electron densities which was invoked in Ref. 21 to explain beatings in the SdH oscillations.

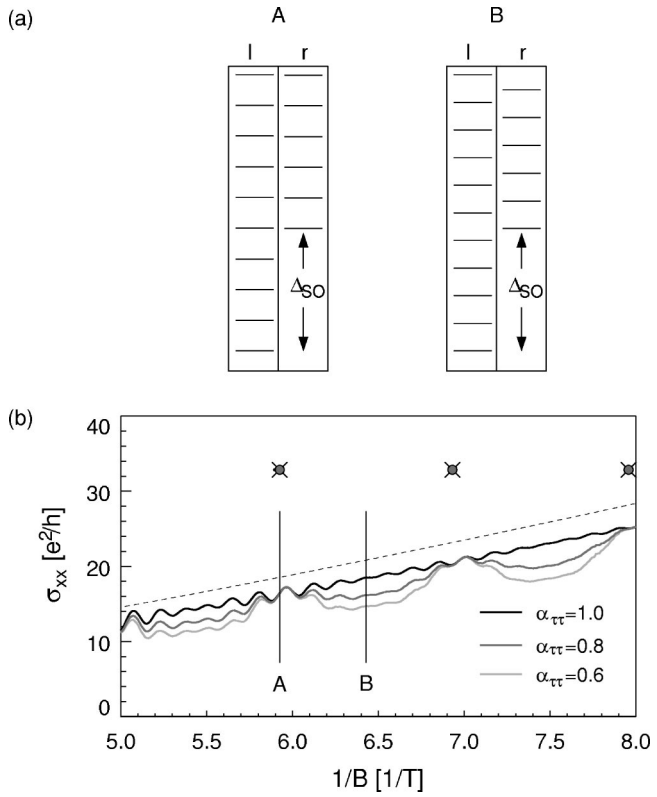

FIG. 4. (a) Sketch of Landau-level spectrum with (A) and without (B) degeneracy of states with different helicity. (b) Longitudinal magnetoconductivity in dependence on the strength of the SO coupling expressed by the parameter $\alpha_{\kappa\kappa}$ for high temperature $T = 3.0$ K. The parameters are those of Fig. 3 and the dashed line is again the classical limit of the SCBA when the Landau levels are decoupled.

V. MAGNETOTRANSPORT IN LATERAL SUPERLATTICES WITH SPIN-ORBIT COUPLING

Lateral semiconductor superlattices have proven to be well suited for studying the physics of Bloch electrons in

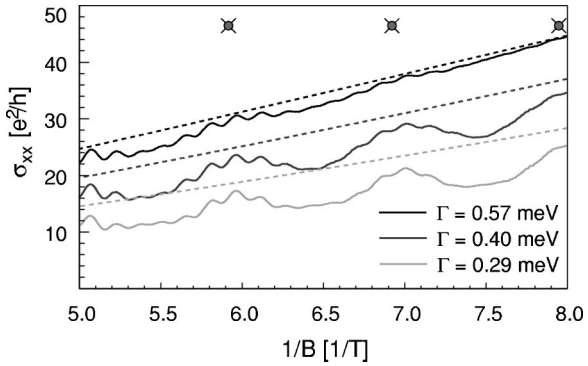

FIG. 5. Longitudinal magnetoconductivity at fixed $\alpha_{rr} = 0.6$ but with different Γ at $T = 3.0$ K. The other parameters are those of Fig. 3. The dashed lines mark the classical limit of the SCBA with decoupled Landau levels.

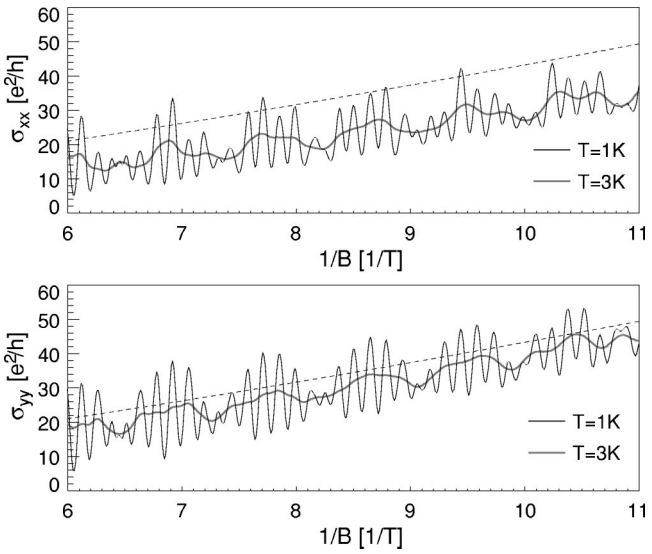

FIG. 6. Longitudinal magnetoconductivities σ_{xx} and σ_{yy} for a lateral superlattice with unidirectional modulation in x direction. Modulation amplitude $V_0=3$ meV, lattice constant $a=75$ nm, Fermi energy $E_F=30$ meV, mobility $\mu=50$ m^2/Vs, and InAs effective mass $m^*=0.0229\,m_e$. The SO coupling is $\alpha_z=2.0\times10^{-11}$ eVm and the mixing coefficient $\alpha_{\kappa\kappa}=0.5$.

artificial periodic systems.[22] A variety of oscillations have been observed in magnetotransport experiments for systems, in which the lattice constant a is comparable with achievable magnetic lengths $\lambda_c=\sqrt{\hbar/eB}$ and both being much smaller (at low temperature) than the carrier mean free path. After having studied the SdH oscillations in the preceding section we focus here on the influence of the Rashba SO interaction on the various magnetoconductivity oscillations due to the periodic modulation mentioned in the Introduction. For the lateral superlattice with Rashba SO interaction the Hamiltonian is given by

$$H=\begin{pmatrix} \frac{1}{2m^*}(\pi_x^2+\pi_y^2) & \frac{\alpha_z}{\hbar}(\pi_x+i\pi_y) \\ \frac{\alpha_z}{\hbar}(\pi_x-i\pi_y) & \frac{1}{2m^*}(\pi_x^2+\pi_y^2) \end{pmatrix} + \begin{pmatrix} V(x,y) & 0 \\ 0 & V(x,y) \end{pmatrix}. \tag{28}$$

We consider here a periodic modulation in x direction described by

$$V(x)=\frac{V_0}{2}\cos\left(\frac{2\pi}{a}x\right). \tag{29}$$

It removes the degeneracy of the Landau levels and is taken into account in evaluating the Kubo formula together with the spin-conserving impurity scattering in the extension of the SCBA as for the homogeneous 2DES. In Fig. 6 the longitudinal magnetoconductivities σ_{xx} and σ_{yy}, in the direction of the modulation and perpendicular to it, respectively, are depicted for potential parameters $V_0=3$ meV, $a=75$ nm, and two temperatures. The Fermi energy was fixed to $E_F=30$ meV, much larger than the amplitude of the periodic potential, which defines the weak modulation case. The mixing coefficient was fixed to the maximum value $\alpha_{\kappa\kappa}=\frac{1}{2}$. Different types of oscillations can be identified of which at the higher temperature (3 K) only the commensurability oscillations and the modulation due to SO coupling survive. The periods (seen in the 1 K traces) can be quantified in simplified models. Following Onsager[31] the SdH periods are

$$\Delta_{1/B}^{\mathrm{SdH:}+/-}=\frac{e\hbar}{m^*\left(E_\mathrm{F}\pm\frac{1}{2}\Delta_\mathrm{SO}\right)}, \tag{30}$$

where the appearance of two Fermi contours due to the spin-splitting is accounted for.[20] The period of the commensurability oscillations in given by[27]

$$\Delta_{1/B}^{\mathrm{CO:}+/-}=\frac{ea}{2\sqrt{2m^*\left(E_\mathrm{F}\pm\frac{1}{2}\Delta_\mathrm{SO}\right)}}, \tag{31}$$

where again the spin-split Fermi contours are considered. The periods reflecting the formation of the miniband structure due to the periodic potential[25,32,33] are quantified by

$$\Delta_{1/B}=\frac{2\pi e}{\hbar}\frac{1}{A}, \tag{32}$$

where A is the cross section of the modified Fermi contour given in Ref. 33. Again the spin splitting due to SO coupling is to be considered and Eq. (32) yield two periods for the Fermi cross sections

$$A^{\mathrm{1D:}+/-}=\frac{2m^*\left(E_\mathrm{F}\pm\frac{1}{2}\Delta_\mathrm{SO}\right)\pi}{\hbar^2} -2\left(\frac{\pi}{a}\right)\sqrt{\frac{2m^*\left(E_\mathrm{F}\pm\frac{1}{2}\Delta_\mathrm{SO}\right)}{\hbar^2}-\left(\frac{\pi}{a}\right)^2} \tag{33}$$

$$-\frac{4m^*\left(E_\mathrm{F}\pm\frac{1}{2}\Delta_\mathrm{SO}\right)}{\hbar^2}\arcsin\frac{\pi\hbar}{a\sqrt{2m^*\left(E_\mathrm{F}\pm\frac{1}{2}\Delta_\mathrm{SO}\right)}}. \tag{34}$$

Finally we may conclude from the eigenvalues of Eq. (8) for $n\gg1$ a period of

$$\Delta_{1/B}^{\mathrm{SO}}=\frac{e\hbar}{m^*\Delta_\mathrm{SO}} \tag{35}$$

for the modulation connected with the crossing points of the Landau levels at the Fermi energy.

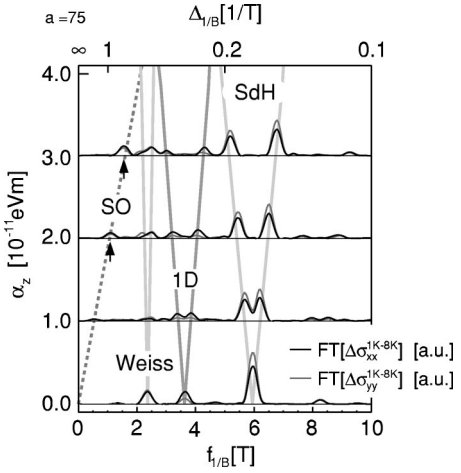

FIG. 7. The absolute value of the Fourier spectrum of the difference of the conductivities at 1 K and 8 K analogous to Fig. 6 is shown in dependence on α_z. The arrows mark the contribution due to the crossing of Landau levels. The calculated Fourier spectrum is compared with the models of Eqs. (30), (31), (32), and (35).

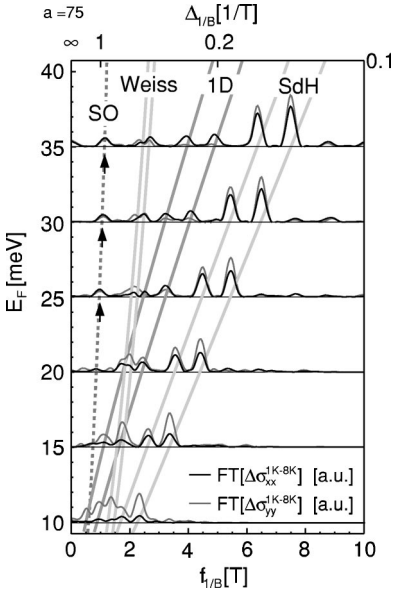

FIG. 8. The absolute value of the Fourier spectrum of the difference of the conductivities at 1 K and 8 K analogous to Fig. 6 is shown in dependence on the Fermi energy E_F. The arrows mark the contribution due to the crossing of Landau levels. Comparison with Eqs. (30), (31), (32), and (35) is shown by straight lines.

In order to analyze all these oscillations we take the power spectrum of the differences $\Delta\sigma_{\mu\mu}$, $\mu=x,y$, of the calculated longitudinal conductivities at 1 K and 8 K. It is shown in dependence on the strength of the SO coupling (Fig. 7) and on the Fermi energy E_F (Fig. 8) together with the periods predicted from Eqs. (30)–(35). In Fig. 7 we see that with increasing SO coupling the frequencies of all (but one) resolved 1/B periodic oscillations split and the maxima of the Fourier transform follow the predictions of the simplified models. This is not the case for the peaks showing up at the lowest $f_{1/B}$ values. These peaks, being due to the modulation resulting from our extension of the SCBA (Sec. III), do not split and follow the analytic expressions of Eq. (35). In Fig. 8 the oscillation period is shown in dependence on the Fermi energy. Again the maxima of our full quantum-mechanical calculation follow the predictions of the simplified models of Eqs. (30)–(35).

VI. SUMMARY

We have calculated the magnetoconductivity for a homogeneous 2DES with spin-orbit interaction including a non-trivial extension of the SCBA which takes into account the spin degree of freedom. The crossing of Landau levels with different helicity, which is induced by the spin-orbit interaction, manifests itself in an additional modulation of the conductivity. It is due to a modification of impurity scattering in the presence of SO coupling. This signature could be used—besides the beating of SdH oscillations—for the experimental verification of SO coupling.

Further we have investigated the influence of SO interaction on the magnetoconductivity oscillations in 1D lateral superlattices. The prediction of the frequencies by simple models and the numerical calculations are in agreement and should motivate an experimental verification.

ACKNOWLEDGMENT

This work has been supported by the DFG via Forschergruppe 370 *Ferromagnet-Halbleiter-Nanostrukturen*.

*Electronic address:
michael.langenbuch@physik.uni-regensburg.de
†Present address: Fraunhofer Institut Naturwissenschaftlich-Technische Trendanalysen, Appelsgarten 2, 53879 Euskirchen, Germany.

[1] É.I. Rashba, Sov. Phys. Solid State **2**, 1109 (1960).
[2] Yu.A. Bychkov and É.I. Rashba, JETP Lett. **39**, 78 (1984).
[3] S.A. Wolf, D.D. Awschalom, R.A. Buhrman, J.M. Daughton, S. von Molnár, M.L. Roukes, A.Y. Chtchelkanova, and D.M. Treger, Science **294**, 1488 (2001).
[4] G. Dresselhaus, Phys. Rev. **100**, 580 (1955).
[5] L. Wissinger, U. Rössler, R. Winkler, B. Jusserand, and D. Richards, Phys. Rev. B **58**, 15 375 (1998).
[6] F.G. Pikus and G.E. Pikus, Phys. Rev. B **51**, 16 928 (1995).
[7] Ch. Schierholz, R. Kürsten, G. Meier, T. Matsuyama, and U. Merkt, Phys. Status Solidi B **233**, 436 (2002).
[8] G.E. Pikus and A.N. Titkov, in *Optical Orientation*, edited by F. Meier and B.P. Zakharchenya (North-Holland, Amsterdam, 1984).
[9] M.I. Dyakonov and V.I. Perel, Sov. Phys. Solid State **13**, 3023 (1972).
[10] N.S. Averkiev and L.E. Golub, Phys. Rev. B **60**, 15582 (1999).
[11] J. Kainz, U. Rössler, and R. Winkler, Phys. Rev. B **68**, 075322 (2003).
[12] S.D. Ganichev, S.N. Danilov, V.V. Bel'kov, E.L. Ivchenko, M. Bichler, W. Wegscheider, D. Weiss, and W. Prettl, Phys. Rev.

Lett. **88**, 057401 (2002).
[13] G. Lommer, F. Malcher, and U. Rössler, Phys. Rev. Lett. **60**, 728 (1988).
[14] J. Nitta, T. Akazaki, H. Takayanagi, and T. Enoki, Phys. Rev. Lett. **78**, 1335 (1997).
[15] J.P. Heida, B.J. van Wees, J.J. Kuipers, T.M. Klapwijk, and G. Borghs, Phys. Rev. B **57**, 11 911 (1998).
[16] Th. Schäpers, G. Engels, J. Lange, Th. Klocke, M. Hollfelder, and H. Lüth, J. Appl. Phys. **98**, 4324 (1998).
[17] C.-M. Hu, J. Nitta, T. Akazaki, H. Takayanagai, J. Osaka, P. Pfeffer, and W. Zawadzki, Phys. Rev. B **60**, 7736 (1999).
[18] E.A. de Andrada e Silva, G.C. La Rocca, and F. Bassani, Phys. Rev. B **50**, 8523 (1994).
[19] R. Winkler, S.J. Papadakis, E.P. De Poortere, and M. Shayegan, Phys. Rev. Lett. **84**, 713 (2000).
[20] S. Keppeler and R. Winkler, Phys. Rev. Lett. **88**, 046401 (2002).
[21] S. Brosig, K. Ensslin, R.J. Warburton, C. Nguyen, B. Brar, M. Thomas, and H. Kroemer, Phys. Rev. B **60**, R13989 (1999).
[22] D. Weiss, Adv. Solid State Phys. **31**, 341 (1991).
[23] D. Weiss, K. von Klitzing, K. Ploog, and G. Weimann, Europhys. Lett. **8**, 179 (1989); R.W. Winkler, J.P. Kotthaus, and K. Ploog, Phys. Rev. Lett. **62**, 1177 (1989).
[24] C. Albrecht *et al.*, Phys. Rev. Lett. **83**, 2234 (1999).
[25] R.A. Deutschmann, W. Wegscheider, M. Rother, M. Bichler, G. Abstreiter, C. Albrecht, and J.H. Smet, Phys. Rev. Lett. **86**, 1857 (2001).
[26] M. Langenbuch, M. Suhrke, and U. Rössler, J. Supercond. **16**, 229 (2003).
[27] L.L. Magarill, Superlattices Microstruct. **16**, 257 (1994).
[28] J. Luo, H. Munekata, F.F. Fang, and P.J. Stiles, Phys. Rev. B **41**, 7685 (1990).
[29] T. Ando, A.B. Fowler, and F. Stern, Rev. Mod. Phys. **54**, 437 (1982).
[30] R.R. Gerhardts, Z. Phys. B **22**, 327 (1975).
[31] L. Onsager, Phys. Rev. **37**, 405 (1931).
[32] C. Albrecht, J.H. Smet, D. Weiss, K. von Klitzing, V. Umansky, and H. Schweizer, Physica B **249-251**, 914 (1998).
[33] M. Langenbuch, R. Hennig, M. Suhrke, U. Rössler, C. Albrecht, J.H. Smet, and D. Weiss, Physica E (Amsterdam) **6**, 565 (2000).